

## Electrochemical Growth of Highly Oriented Organic–Inorganic Superlattices Using Solid-Supported Multilamellar Membranes as Templates

Li-Li Xing,<sup>†</sup> Da-Peng Li,<sup>†</sup> Shu-Xin Hu,<sup>†</sup> Huai-Yu Jing,<sup>†</sup> Honglan Fu,<sup>‡</sup>  
Zhen-Hong Mai,<sup>†</sup> and Ming Li<sup>\*†</sup>

Contribution from the Beijing National Laboratory for Condensed Matter Physics, Institute of Physics, Chinese Academy of Sciences, Beijing 100080, P. R. China, and College of Life Science, Peking University, Beijing 100871, P. R. China

Received September 19, 2005; E-mail: mingli@aphy.iphy.ac.cn

**Abstract:** Controllable depositing of relatively thick inorganic sublayers into organic templates to fabricate organic–inorganic superlattices is of great importance. We report a novel approach to fabricating phospholipid/Ni(OH)<sub>2</sub> superlattices by electrochemical deposition of the inorganic component into solid-supported multilamellar templates. The well-ordered and highly oriented multilamellar templates are produced by spreading small drops of lipid solution on silicon surfaces and letting the solvent evaporate slowly. The templates which are used as working electrodes preserve the lamellar structure in the electrolyte solution. The resulting superlattices are highly oriented. The thickness of the nickel hydroxide is controlled by the concentration of nickel ions in the electrolyte bath. The electron density profiles derived from the X-ray diffraction data reveal that the thickness of the nickel hydroxide sublayers increases from 15 to 27 Å as the concentration of nickel nitrate increases from 0.005 mol/L to 0.08 mol/L. We expect that the new method can be extended to depositing a variety of inorganic components including metals, oxides, and semiconductors.

### Introduction

Complex systems consisting of organic and inorganic components have great potential for the creation of new kinds of functional material by utilizing the wide variety of properties exhibited by each component.<sup>1–7</sup> Their unique electronic, magnetic, and photonic properties have inspired chemists and materials scientists to develop synthetic, biomimetic nanocomposite assemblies.<sup>7–20</sup> Nevertheless, the efficient processing of organic–inorganic superlattices (OISLs) remains an elusive

goal, especially when a high degree of orientation is required. Oriented ZnO-surfactant hybrid multilayers were electrochemically self-assembled on silicon substrates from Zn(NO<sub>3</sub>)<sub>2</sub> solutions containing surfactant.<sup>8,9</sup> It seemed very hard to make the metal oxide sublayers thicker than a half nanometer. Metal ions (Cd<sup>2+</sup>, Pb<sup>2+</sup>, etc.) in Langmuir–Blodgett films were reacted with chalcogenide gas (e.g., H<sub>2</sub>S) to yield nanometer-sized inorganic clusters.<sup>10</sup> But to the best of our knowledge, no report has ever been given to clearly show that such a reaction would not disrupt the lamellar structure when the nanoclusters grow larger. Nor is there a report to show that homogeneous inorganic layers rather than discrete clusters were formed inside the templates. Using silica and surfactant as precursors, organic–inorganic nanocomposites on solid substrates were fabricated by evaporation-induced self-assembly.<sup>11,21</sup> Although continuous films can be obtained with this technique, it applies only to a certain class of inorganic reagents. Fabricating large area and high quality OISLs remained to be a great challenge.

Lipids play an important role in biomineralization and other biological processes. Self-assembled structures of lipids can serve as templates for chemical reactions because the headgroups

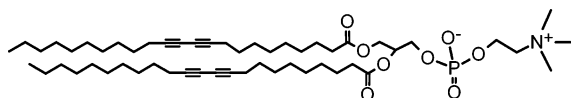
<sup>†</sup> Chinese Academy of Sciences.

<sup>‡</sup> Peking University.

- (1) Aksay, I. A.; Trau, M.; Manne, S.; Honma, I.; Yao, N.; Zhou, L.; Fenter, P.; Eisenberger, P. M.; Gruner, S. M. *Science* **1996**, *273*, 892–898.
- (2) Whitesides, G. M.; Mathias, J. P.; Seto, C. T. *Science* **1991**, *254*, 1312–1319.
- (3) Lopes, W. A.; Jaeger, H. M. *Nature* **2001**, *414*, 735–738.
- (4) Takada, J.; Awaji, H.; Koshioka, M.; Nakajima, A.; Nevin, W. A. *Appl. Phys. Lett.* **1992**, *61*, 2184–2186.
- (5) Nandhakumar, I. S.; Gabriel, T.; Li, X.; Attard, G. S.; Markham, M.; Smith, D. C.; Baumberg, J. J. *Chem. Commun.* **2004**, *12*, 1374–1375.
- (6) Li, L.; Stupp, S. I. *Angew. Chem., Int. Ed.* **2005**, *44*, 1833–1836.
- (7) Braun, P. V.; Osenar, P.; Stupp, S. I. *Nature* **1996**, *380*, 325–328.
- (8) Jing, H.-Y.; Li, X.-L.; Lu, Y.; Mai, Z.-H.; Li, M. J. *Phys. Chem. B* **2005**, *109*, 2881–2884.
- (9) Choi, K.-S.; Lichtenegger, H. C.; Stucky, G. D.; McFarland, E. W. *J. Am. Chem. Soc.* **2002**, *124*, 12402–12403.
- (10) Ichinose, I.; Kimizuka, N.; Kunitake, T. *J. Phys. Chem.* **1995**, *99*, 3736–3742.
- (11) Sellinger, A.; Weiss, P. M.; Nguyen, A.; Lu, Y.; Assink, R. A.; Gong, W.; Brinker, C. J. *Nature* **1998**, *394*, 256–260.
- (12) Stupp, S. I.; Braun, P. V. *Science* **1997**, *277*, 1242–1248.
- (13) Hartgerink, J. D.; Beniash, E.; Stupp, S. I. *Science* **2001**, *294*, 1684–1688.
- (14) Decher, G. *Science* **1997**, *277*, 1232–1237.
- (15) Tokito, S.; Sakata, J.; Taga, Y. *Appl. Phys. Lett.* **1994**, *64*, 1353–1355.
- (16) Attard, G. S.; Bartlett, P. N.; Coleman, N. R. B.; Elliott, J. M.; Owen, J. R.; Wang, J. H. *Science* **1997**, *278*, 838–840.

- (17) Nelson, P. A.; Elliott, J. M.; Attard, G. S.; Owen, J. R. *Chem. Mater.* **2002**, *14*, 524–529.

- (18) Markham, M. L.; Baumberg, J. J.; Smith, D. C.; Li, X.; Gabriel, T.; Attard, G. S.; Nandhakumar, I. *Appl. Phys. Lett.* **2005**, *86*, Art. No. 011912.
- (19) Gabriel, T.; Nandhakumar, I. S.; Attard, G. S. *Electrochem. Commun.* **2002**, *4*, 610–612.
- (20) Attard, G. S.; Leclerc, S. A. A.; Maniguet, S.; Russell, A. E.; Nandhakumar, I.; Bartlett, P. N. *Chem. Mater.* **2001**, *13*, 1444–1446.
- (21) Ogawa, M. *J. Am. Chem. Soc.* **1994**, *116*, 7941–7942.

**Scheme 1.** Structure of DC<sub>8,9</sub>PC

of lipids are materially compatible with inorganic reactants. The template can guide the growth of oriented crystals of specific structure, size, and morphology through the process of molecular recognition at the interfaces.<sup>22</sup> The lipid assemblies are therefore receiving increasing attention for the synthesis of new biomimetic materials. They are simple and versatile nucleants for inorganics because the nucleating functionalities and their interfacial organization can be controlled by the appropriate choice of amphiphile and thermodynamic parameters.

Phospholipids can readily self-assemble into lamellar structures. An easy and efficient way to form well ordered multilamellar bilayers is to spread a small drop of lipid solution on a solid substrate.<sup>23</sup> Highly oriented multilayers of phospholipids can be produced after slow evaporation of the solvent. The overall film thickness  $D$  ranges from 50 nm to 10  $\mu\text{m}$ , depending on the amount of lipids used in the initial spreading. The quality of the multilayers can be even higher than Langmuir–Blodgett films. For instance, samples with domain sizes larger than 40  $\mu\text{m}$  in the lateral direction and with extremely low mosaicity (less than  $5 \times 10^{-3}$  degrees) have been reported.<sup>24</sup> The interheadgroup spaces in the phospholipid multilayers can be readily filled with aqueous solutions, facilitating the growth of various inorganic compounds inside.

In this article, we report on a novel approach to constructing OISLs by growing nickel hydroxide in the interheadgroup spaces of the phospholipid bilayers. The technique uses solid-supported phospholipid multilayers as templates to direct the growth of inorganic sublayers. We adopt the electrochemical method to reduce the inorganic precursors because it is flexible, versatile, and easy to operate. The structural quality of the template is very high with all their interfaces being parallel to the surface of the substrate. The lamellar structure of the template is preserved in electrolyte solutions of low ionic strength. The resulting OISLs are highly oriented with low mosaicity. The periodicity of the superlattices can be changed by adjusting the concentration of the electrolyte in the electrochemical cell.

## Experimental Section

**Chemicals.** The polymerizable phospholipid 1,2-bis(10,12-tricosadiynoyl)-*sn*-glycero-3-phosphocholine (DC<sub>8,9</sub>PC, Scheme 1) was purchased from Avanti Polar Lipids and used without further purification. Nickel nitrate hexahydrate ( $\text{Ni}(\text{NO}_3)_2 \cdot 6\text{H}_2\text{O}$ ) and poly(ethylene glycol) (PEG, MW = 400 from Sigma) are analytical reagent grade and were used as received. Distilled water ( $>18 \text{ M}\Omega \cdot \text{cm}$ ) was produced using a Millipore filter system.

**DC<sub>8,9</sub>PC Multilayers.** The DC<sub>8,9</sub>PC multilayers were prepared on hydrophilic silicon substrates. P-type, (100)-oriented silicon wafers with a resistance of 0.01  $\Omega \cdot \text{cm}$  were cleaned ultrasonically in acetone and ethanol for about 3 min. They were then boiled in a mixture of  $\text{H}_2\text{O}/\text{H}_2\text{O}_2/\text{H}_2\text{SO}_4 = 5:1:1$  (by volume) for 20 min and boiled again in a mixture of  $\text{H}_2\text{O}/\text{H}_2\text{O}_2/\text{NH}_3 \cdot \text{H}_2\text{O} = 5:1:1$  (by volume) for 20 min. The wafers were finally rinsed with pure water and dried in a stream of

nitrogen before use. The DC<sub>8,9</sub>PC powder was dissolved in a mixture of methanol and chloroform [1 mg/(50  $\mu\text{L}$  + 50  $\mu\text{L}$ )] and pipetted onto the silicon substrate (1.5 cm  $\times$  1.5 cm) in a chamber. The solution spreads spontaneously, and the solvent evaporated slowly over a period of 6 h. The samples were then kept in a vacuum desiccator for another 12 h to get rid of any residual solvent. It can be estimated that each film contains about 350 bilayers according to the area per molecule, the total spread area, and the volume of the solution pipetted. The membranes polymerized by irradiating the samples with UV light (254 nm) for 10 min.

**Electrodeposition.** The electrodeposition was performed on a CHI660A electrochemical station, using a homemade three-electrode cell with the template-covered silicon as the working electrode, a platinum sheet as the counter electrode, and a saturated calomel electrode (SCE) as the reference electrode. The electrical contact was realized by painting conducting silver paste on the rear side of the silicon wafer. The electrochemical cell contains  $\text{Ni}(\text{NO}_3)_2$  solution with 25 wt % poly(ethylene glycol) additive. Nickel hydroxide was deposited inside the multilayer using the double potential step mode. The potential was altered repeatedly between two values ( $E_1 = -1.3 \text{ V}$  and  $E_2 = 0 \text{ V}$  versus SCE). The total deposition time depends on the thickness of the template, which is about 2  $\mu\text{m}$  in this work. It took about 17 h for all the interheadgroup spaces to be filled with the inorganics.

**Characterization.** The lamellar structure of the superlattices was characterized by the low-angle X-ray diffraction on a 5-circle Huber diffractometer on the 4W1A beam line at the Beijing Synchrotron Radiation Facility. Monochromatic radiation was selected by a triangular bent Si (220) crystal. The wavelength of the X-rays is  $0.154 \pm 0.001 \text{ nm}$ . The vertical and horizontal angular divergences of the focused X-ray beam are  $0.02^\circ$  and  $0.08^\circ$ , respectively. The incident beam was further confined by a 0.1 mm slit 400 mm before the sample and the scattered beam was confined by a 0.2 mm slit. The diffraction data were collected by performing the  $\theta/2\theta$  scans while keeping the incidence angle equal to the exiting angle. The rocking curves around the Bragg points were used to characterize the degree of orientation of the multilayers. They were measured by rocking the samples, but keeping the angle between the incidence and the reflection fixed. The crystallographic structure of the inorganic component was studied by the glancing-angle X-ray diffraction, in which the incident angle between the X-ray beam and the sample surface was fixed at  $0.3^\circ$  while the intensity of the scattered X-rays was monitored as a function of the  $2\theta$  angle.

The surface morphology of the films was imaged by a Hitachi S-4200 scanning electron microscope (SEM) and by a NanoScope IIIa-D3000 atomic force microscope (AFM). Specimens for transmission electron microscopy (TEM) were scraped from the silicon substrate with a razor blade. They were embedded into ethoxy at  $70^\circ\text{C}$ . After about 11 h the polymerized block was cut into thin slices of  $\sim 60 \text{ nm}$  thick. The thin slices were then fixed on carbon-coated copper grids. The observations were undertaken with a JEOL JEM-100CX II electron microscope operated at 100 kV.

## Results and Discussions

Before electrodeposition the solid-supported multilayer was incubated in the electrochemical cell for about 1 h, during which the multilayer swelled to the fully hydrated state with the interheadgroup spaces being filled with nickel nitrate solution. At this stage the multilayer is in a lamellar liquid crystalline state, similar to the liquid crystal templates used by Attard et al.<sup>5,16–20</sup> The difference between Attard's method and ours is that the total amount of the inorganic reagents in their hexagonal liquid crystals was defined before electrodeposition, while the inorganic reagents in our multilamellar templates are supplied by the solution in the electrochemical cell and therefore can be partly renewed after being consumed by the electrodeposition

(22) Kmetko, J.; Yu, C.; Eymenenko, G.; Kewalramani, S.; Dutta, P. *Phys. Rev. Lett.* **2002**, *89*, Art. No. 186102.

(23) Seul, M.; Sammon, M. J. *Thin Solid Films* **1990**, *185*, 287–305.

(24) Vogel, M.; Münster, C.; Fenzl, W.; Thiaudiere, D.; Salditt, T. *Physica B* **2000**, *283*, 32–36.

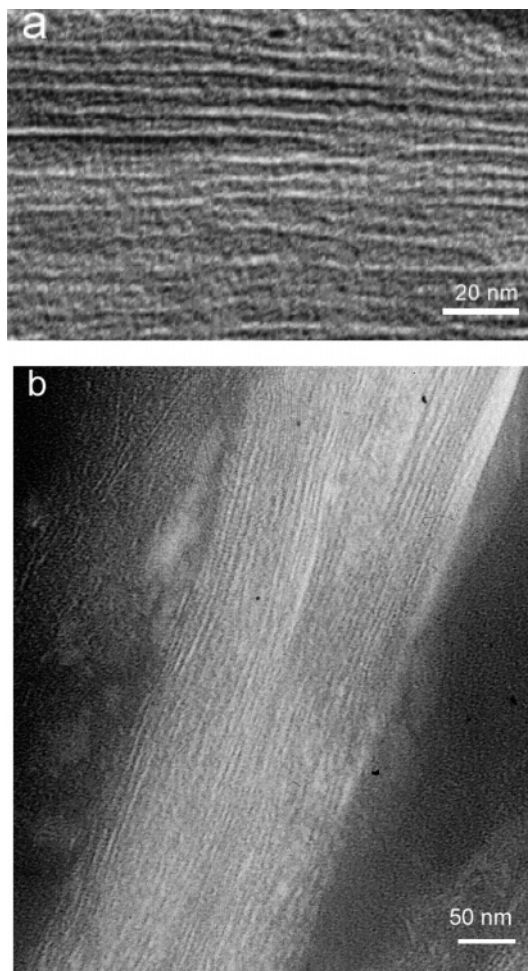


**Figure 1.** TEM images of the superlattices electrodeposited from (a) 0.005 mol/L and (b) 0.05 mol/L nickel nitrate solutions using the DC<sub>8,9</sub>PC multilayers as templates.

process. The total amount of the reduced ions can therefore be larger than that initially stored in the interheadgroup spaces. The PEG additive (25 wt %) in the solutions increases the osmotic pressure so that the peeling-off of the DC<sub>8,9</sub>PC bilayers can be sufficiently suppressed. This trick is important because otherwise the top bilayers would eventually peel-off from the multilayers to destroy the integrality of the templates. The bilayers play an active role as the structural template to direct the heterogeneous condensation of the inorganic crystalline component. At  $E_1 = -1.3$  V versus SCE, nitrate ions are reduced and hydroxide ions are generated. The hydroxide ions increase the local pH value so that nickel hydroxide precipitates are produced. The corresponding cathodic reaction equations of the electrochemical process are (1)  $\text{NO}_3^- + \text{H}_2\text{O} + 2e^- \rightarrow \text{NO}_2^- + 2\text{OH}^-$  and (2)  $\text{Ni}^{2+} + 2\text{OH}^- \rightarrow \text{Ni}(\text{OH})_2\downarrow$ . The reaction starts from the interface between the first bilayer and the substrate, where the electrochemically generated hydroxide ions combine immediately with the nickel ions around them. The nickel hydroxide precipitates fill the first interface very soon. The growth front is then moved to the next interface at which hydroxide ions are produced locally to combine with the nickel ions. The growth front moves interface by interface until, finally, it moves out toward the topmost interface.

The TEM images in Figure 1 show clearly that the superlattices have a well defined lamellar nanostructure with continu-

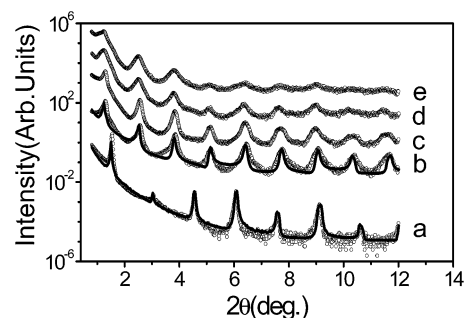


**Figure 2.** Low-angle X-ray diffraction patterns of the films deposited with different nickel nitrate concentrations: (b) 0.005, (c) 0.01, (d) 0.03, and (e) 0.05 mol/L. Curve a is the diffraction pattern of the template.

ous nickel hydroxide layers intercalated between the lipid bilayers. The distribution of the stacking direction of the sublayers is narrow. The main defects are dislocations which were copied from the templates. Since the electrodeposition process does not destroy the integrality of the multilamellar templates, no significant defects are newly created. The observed local fluctuation of the sublayers and local variation of the interbilayer distances are intrinsic of phospholipid multilayers.<sup>24</sup> They may also arise from fluctuations of the concentration of ions inside the interheadgroup spaces during the electrodeposition. A rough estimate of the mean periodicity of the superlattice and thickness of the nickel hydroxide gives values in the ranges 6–8 nm and 1–3 nm, respectively. These values are further refined by the low angle X-ray diffraction.

Figure 2 is the low-angle X-ray diffraction patterns of typical samples measured under ambient conditions (25 °C and 35% relative humidity). The as-cast DC<sub>8,9</sub>PC multilayer is highly ordered as can be seen from the sharp Bragg peaks (curve a). Its stacking period is  $56.9 \pm 0.2$  Å. The lamellar structure is not disrupted by the electrodeposition process. For the highest nickel nitrate concentration used (0.08 mol/L) the period of the lamellar structure becomes  $78.7 \pm 0.4$  Å, the inorganic sublayer of which is about 27 Å. Template-directed growth of OISLs with such thick inorganic sublayers has not been reported previously.

The low-angle X-ray diffraction is sensitive to the electron density profile (EDP)  $\rho(z)$  of the bilayer. The EDP can be obtained by theoretical simulation of the diffraction data.<sup>25</sup> Alternatively, it can be refined via

$$\rho(z) = \sum_1^M f(q_m) \cos(2\pi mz/d) \quad (1)$$

where  $f(q_m)$  is the form factor of the bilayer,  $d$  is the period of the multilayer, and  $m$  running from 1 to  $M$  is the index of the Bragg peaks.<sup>26</sup> The magnitudes of  $f(q_m)$  are determined from the intensities at the Bragg peaks,

$$I(q) \propto \left| \sum_0^N f_n e^{iqnd} \right|^2 / q^2 \quad (2)$$

where  $f_0 = f_S$  is the reflection of the substrate and  $f_n = f(q) \exp(-idq/2)$ . Due to the mirror plane symmetry of the bilayers, the phases of  $f(q_m)$  are reduced to their positive/negative signs only, facilitating the phase problem enormously.<sup>26</sup> The method has been widely used to refine the structure of phospholipid

(25) *X-ray Scattering from Soft-Matter Thin Films*; Tolan, M.; Hohler, G., Eds.; Springer-Verlag: Karlsruhe, 1999.

(26) Hu, S.-X.; Li, X.-H.; Jia, Q.-J.; Mai, Z.-H.; Li, M. *J. Chem. Phys.* **2005**, *122*, Art. No. 124712.

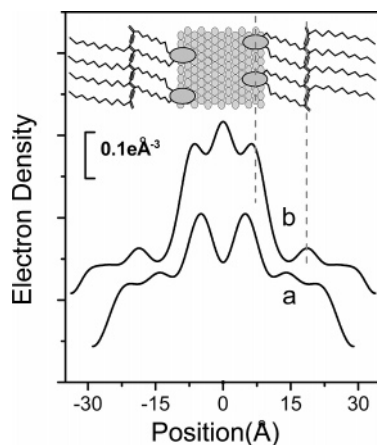


**Figure 3.** Electron density profiles of an as-cast multilayer (a) and an OISL deposited from 0.005 mol/L nickel nitrate solution (b). Inset is the corresponding molecular model of a period of the OISL.

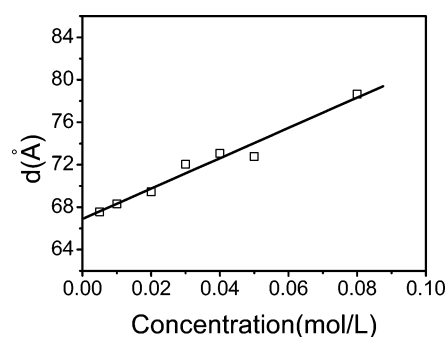
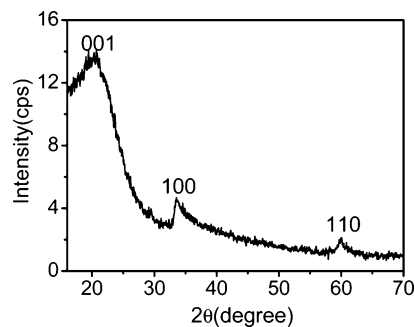


**Figure 4.** Period of the superlattices increases linearly with the nickel nitrate concentration in the electrolyte bath.

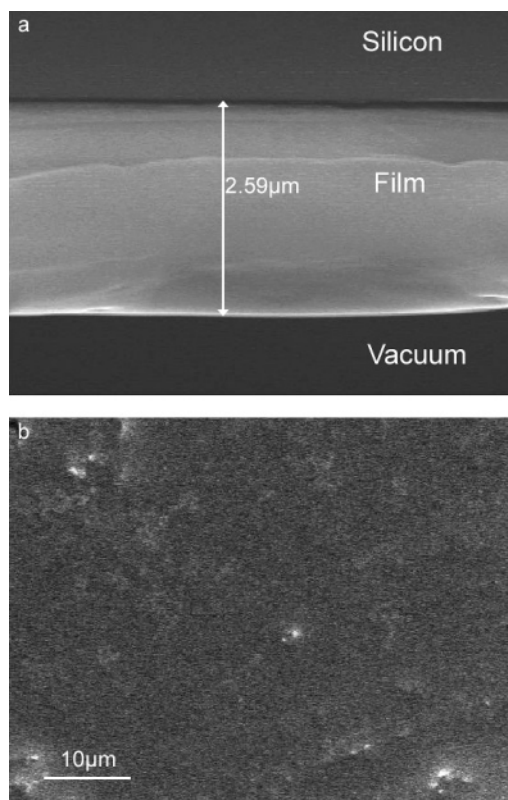
bilayers. It has the advantage that the ambiguity introduced by model simulation can be greatly reduced. Using the algorithm introduced in ref 26, we obtained the EDP of the bilayers.

Figure 3 compares the EDP of the as-cast multilayer with the OISLs electrodeposited from 0.005 mol/L nickel nitrate solution. The corresponding theoretical diffraction patterns are drawn in Figure 2 (the solid lines). Our confidence in the correctness of the EDP lies in the fact that the main features are all in accordance with our knowledge of the basic bilayer profiles. For instance, from the EDP of the as-cast multilayer (curve a) one sees clearly the high-density headgroup area (with a water layer of  $\sim 5$  Å between) and the electron-deficient layer formed by the juxtaposition of the hydrophobic ends. Also clear is the electron density of the diacetylene part which is higher than the mean electron density of the saturated alkyl chains. Comparing the EDP before and after the electrodeposition, one sees that the main change is in the central part where nickel hydroxide is intercalated into the multilayer to replace the water so that the central part becomes denser and thicker.

The period of the superlattice increases linearly with the nickel nitrate concentration (Figure 4). Our analysis indicates that the thickness of the inorganic sublayers (within which the headgroups are imbedded) is mainly determined by the concentration of the electrolyte bath. It increases from 15 to 27 Å as the concentration of nickel nitrate is increased from 0.005 to 0.08 mol/L. The inorganic sublayers are thick enough for their crystallographic structure to be determined by high-angle X-ray diffraction. The diffraction pattern of a sample deposited with 0.05 mol/L nickel nitrate is depicted in Figure 5 which can be



**Figure 5.** High angle X-ray diffraction pattern of the inorganic sublayers can be indexed to hexagonal-phased nickel hydroxide.



**Figure 6.** SEM images of an OISL electrodeposited from 0.03 mol/L nickel nitrate solution: (a) cross-section profile; (b) surface profile.

indexed to hexagonal-phased nickel hydroxide. The intrinsic solid-state properties of the inorganic component in an OISL can be well exhibited only when the inorganic sublayer is thick enough not to be disturbed by the interfaces. It is therefore great progress to be able to intercalate relatively thick inorganic sublayers into the organic templates. The ability to control the thickness of the inorganic sublayers is another advantage of our method because, in optoelectronic industry, the energy band of the inorganic solid often needs to be tailored to fit a special application. The most effective way to tailor the energy band is to change their thickness.

The cross-section SEM image of a typical sample (see Figure 6a) reveals that the overall thickness of the OISL is about 2.59  $\mu\text{m}$  which is in good agreement with the estimate that the template is composed of about 350 bilayers. It means that the total thickness of the films can be controlled by varying the lipid concentration of the initial spreading solution. We are able to produce phospholipid multilayers thinner than 50 nm as well

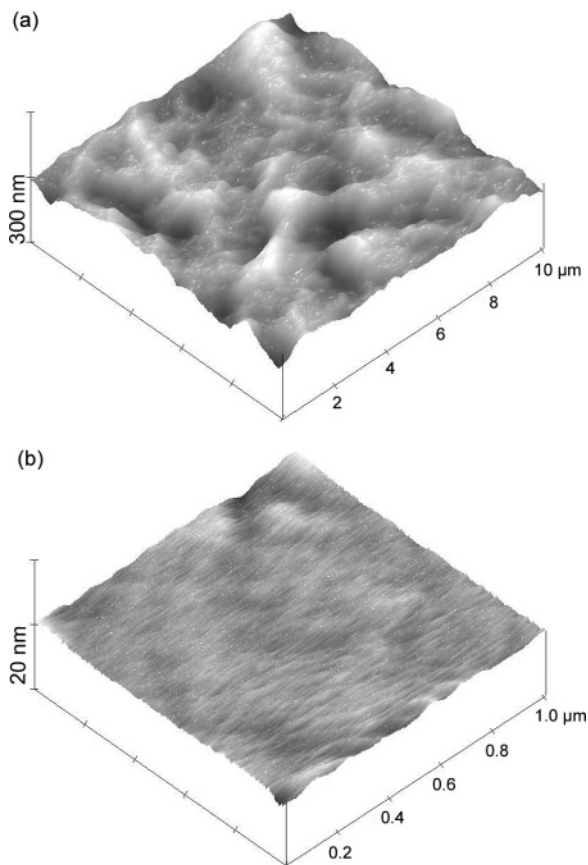


**Figure 7.** AFM surface morphologies of the OISL deposited from 0.03 mol/L nickel nitrate solution.

as that thicker than 5  $\mu\text{m}$ . The surface morphologies of the same OISL imaged by SEM (Figure 6b) and AFM (Figure 7) clearly show that the superlattices are laterally homogeneous and their surfaces are relatively smooth. The root-mean-squared (rms) roughness is about 0.44 nm averaged over an area of  $1 \times 1 \mu\text{m}^2$  and is about 15.5 nm averaged over an area of  $10 \times 10 \mu\text{m}^2$ . The surface morphology of the OISL is quite similar to that of the template (data not shown), meaning that the phospholipid multilayer is very stable. Few holes due to bilayer peeling-off are formed on the surface during the electrodeposition process.

The width and number of the measurable peaks of the low-angle Bragg diffraction and the width of the rocking curves at the Bragg peaks are direct criterions of the overall structural quality of the multilayers.<sup>25</sup> The quality of the fabricated OISL is found to depend on the concentration of nickel nitrate in the electrolyte bath. The lamellar structure becomes less ordered at higher nickel nitrate concentrations. The observation that the Bragg peaks become wider at higher angles is indicative of the variation of the inter-bilayer distances in the superlattices. Nonetheless, up to eight Bragg peaks are observable even for the worst samples we got, implying that the superlattices are structurally coherent over many sublayers. The superlattices are also homogeneous in the lateral direction. Generally speaking, extended defects and/or dislocations may exist in the multilayer. The sample should therefore be treated as a collection of perfect domains in which the sublayers are homogeneous and are parallel to each other. We take the superlattice fabricated from 0.01 mol/L nickel nitrate solution as an example to give an analysis of the lateral extension of the lamellar domains. The

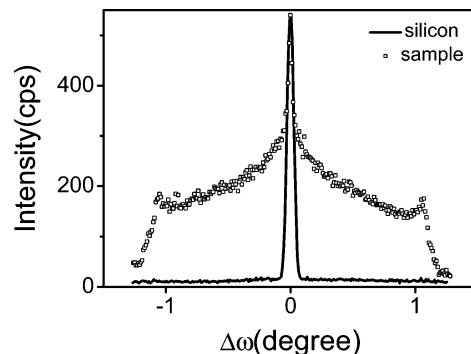


**Figure 8.** The sharp central peak of the rocking curve indicates that the mosaicity of the superlattice is low. The rocking curve of a silicon wafer measured at the same  $2\theta$  angle is also depicted to show that the width of the central peak is limited by the instrumental resolution. The intensities are normalized at the center.

mosaicity of the domains can be directly read from the width of the central peak of the rocking curve (Figure 8). The full width at half-maximum of the central peak is limited by the instrumental resolution, indicating that the mosaicity of the superlattice is very low.<sup>22</sup> The sublayers in the superlattice are therefore highly oriented with all their interfaces being parallel to the surface of the substrate. The central peak also gives the average lateral extension of the lamellar domains.<sup>24,25</sup> When being deconvoluted with the resolution function of the diffractometer and fitted to a Lorentzian curve, it sets a lower limit of about 10  $\mu\text{m}$ .

Control experiments reveal that the period of the OISL does not change monotonically with the concentration of the PEG additive. It implies that the thickness of the deposited inorganic sublayer is not determined by the size of the interheadgroup spaces in solution because the latter does decrease monotonically with the increasing of the osmotic pressure. During the electrocrystallization, the ions in the electrolyte bath diffuse into the interheadgroup spaces to renew the ones already consumed by the electrodeposition process such that the total amount of the reduced ions is larger than that initially stored in the interheadgroup spaces. Under adequate conditions, the deposited inorganic sublayer can be even thicker than the interheadgroup spacing of the fully hydrated multilayer. The extended defects between the domains provide pathways for the ions to enter the multilayer during the electrodeposition process. The ions can also diffuse easily in the lateral direction. The diffusion coefficient in the lateral direction is much larger than the one in the direction perpendicular to the bilayers.<sup>27,28</sup> The growth of an inorganic sublayer in a domain is stopped once all the lateral alleyways for the ions are blocked. In this case, the growth of the inorganic sublayer may be locally incomplete so that the thickness of the bilayers in the superlattice is not as uniform as that in the as-cast multilayer. This explains why the Bragg peaks of the fabricated OISL are wider than those of the as-cast multilayer.

## Conclusions

Using solid-supported phospholipid multilayers as templates, we have fabricated high quality  $\text{Ni}(\text{OH})_2$ /phospholipid super-

(27) Chen, C.; Postlethwaite, T. A.; Hutchison, J. E.; Samulski, E. T.; Murray, R. W. *J. Phys. Chem.* **1995**, *99*, 8804–8811.

(28) Postlethwaite, T. A.; Samulski, E. T.; Murray, R. W. *Langmuir* **1994**, *10*, 2064–2067.

lattices by electrodeposition of  $\text{Ni}(\text{OH})_2$  in the interheadgroup spaces. Three factors make our method different from the ones previously reported in the literature: (1) the solid-supported multilamellar templates are easy to make whose overall thickness can be controlled. The final products are of high quality with their interfaces being all parallel to the surface of the substrate. (2) The templates are immersed in electrolytes which serve as a reservoir for ions during the electrodeposition. The lipid multilayers are soft with the interheadgroup spaces adjustable to the environment. This property is sufficiently utilized in this work to intercalate in a controllable way relatively thick inorganic sublayers into organic templates. And, (3) the concentration of the electrolyte solution is very low so that the templates can remain stable in the electrochemical cell. This point is very important because it is not very easy to produce a stable lamellar lyotropic liquid crystal containing a high concentration of ions, which is needed to produce thick inorganic sublayers by other template-directed growth techniques.

The electrodeposition technique is adopted in this work. It is an ideal way to fill topologically complex structures because it starts from deep within the structure and then grows out toward the exposed surface. It has been widely used to fabricate nanostructured materials via template-directed means. For example, it has been used to fabricate metal and semiconductor particulate films from aqueous solutions of their precursors under Langmuir monolayers.<sup>29,30</sup> It has also been used to produce nanocomposites with well-defined periodic nanostructures, using lyotropic liquid crystals as templates.<sup>5,16–20</sup> We believe that the

method used in this work can be generalized for the following two reasons. (1) The multilamellar templates are fabricated before electrodeposition, being independent of the ions in the electrolytes. The templates can in principle be used to direct the condensation of many inorganics so long as they are materially compatible with the headgroups of bilayers, which should not be a problem because there are many choices for the headgroups. The researchers can always design a specific headgroup to fit the inorganics. (2) Reports have shown that many materials such as metal oxides or even metals can be readily interfaced to lipid headgroups via electrodeposition.<sup>5,16–20,29,30</sup> As we have emphasized, the fully hydrated multilayers are in a liquid crystalline state, similar to the liquid crystal templates in refs 5 and 16–20 which have been used to fabricate different kinds of nanocomposites. We are trying to use the method to deposit a variety of inorganic components including metals, oxides, and semiconductors. Some recent results are shown in the Supporting Information. The quality is presently not as good as what we showed above. The growth mechanism of the new superlattices will be studied further.

**Acknowledgment.** This work was supported by the National Natural Science Foundation of China under Grant 10325419 and by the National Basic Research Program of China under Grant 2004CB619005. The authors thank Mr. Q. J. Jia for his help in the synchrotron X-ray experiment at BSRF.

**Supporting Information Available:** Additional examples of other types of OISLs deposited in a solution of 0.005 mol/L  $\text{NiCl}_2$  and a solution of 0.01 mol/L  $\text{ZnSO}_4$  and 0.005 mol/L  $\text{Na}_2\text{S}_2\text{O}_3$ . This material is available free of charge via the Internet at <http://pubs.acs.org>.

JA056448N

- (29) Kotov, N. A.; Zanicelli, M. E. D.; Meldrum, F. C.; Fendler, J. H. *Langmuir* **1993**, *9*, 3710–3716.  
(30) Saliba, R.; Mingotaud, C.; Argoul, F.; Ravaine, S. *J. Electrochem. Soc.* **2003**, *150*, C175–C183.